Aalto University

OPEN ACCESS

This is an electronic reprint of the original article.
This reprint may differ from the original in pagination and typographic detail.

Tripathi, Tripurari S.; Karppinen, Maarit

Enhanced p-Type Transparent Semiconducting Characteristics for ALD-Grown Mg-Substituted $CuCrO_2$ Thin Films

Published in:
Advanced Electronic Materials

DOI:
10.1002/aelm.201600341

Published: 01/06/2017

Document Version
Peer-reviewed accepted author manuscript, also known as Final accepted manuscript or Post-print

Published under the following license:
Unspecified

Please cite the original version:
Tripathi, T. S., & Karppinen, M. (2017). Enhanced p-Type Transparent Semiconducting Characteristics for ALD-Grown Mg-Substituted $CuCrO_2$ Thin Films. *Advanced Electronic Materials*, *3*(6), Article 1600341. https://doi.org/10.1002/aelm.201600341

This material is protected by copyright and other intellectual property rights, and duplication or sale of all or part of any of the repository collections is not permitted, except that material may be duplicated by you for your research use or educational purposes in electronic or print form. You must obtain permission for any other use. Electronic or print copies may not be offered, whether for sale or otherwise to anyone who is not an authorised user.

Enhanced p-type transparent semiconducting characteristics for ALD-grown Mg-substituted $CuCrO_2$ thin films

*Tripurari S. Tripathi, Maarit Karppinen**

Dr. T. S. Tripathi, Prof. Maarit Karppinen
Department of Chemistry, Aalto University,
P.O. Box 16100, FI-00076 Aalto, Finland
*maarit.karppinen@aalto.fi

Keywords: atomic layer deposition, p-type transparent conducting oxides, delafossites, Magnesium-substituted $CuCrO_2$

Abstract

Magnesium-substituted $CuCrO_2$ delafossite is a promising candidate for p-type transparent conducting oxide (TCO) applications owing to its relatively high electrical conductivity and optical transparency in the visible range. Here we report the ALD (atomic layer deposition) fabrication of semiconducting $Cu(Cr_{1-x}Mg_x)O_2$ (up to x = 0.043) thin films based on $Cu(thd)_2$ (thd = 2,2,6,6-tetramethyl-3,5-heptanedionate), $Cr(acac)_3$ (acac = acetyl acetonate) and $Mg(thd)_2$ as metal precursors and ozone as the oxygen source. Smooth and homogeneous thin films with an accurately controlled Mg content are obtained at the deposition temperature of 250 ^{o}C. A limited substitution level is revealed from X-diffraction patterns: peaks due to the spinel-structured $MgCr_2O_4$ secondary phase appear for $x \geq 0.015$ while the increase in lattice parameters of the delafossite $Cu(Cr,Mg)O_2$ phase continues even up to $x \approx 0.03$. The direct bandgap as determined from UV-vis spectrophotometric measurements is observed to decrease from 3.09 eV for $x = 0$ to 2.87 eV for x = 0.015 before increasing to 3.15 eV for x = 0.043. The observed transmittance is close to 80% in the visible range. These characteristics are superior to the thin films of copper delafossite family prepared by any thin-film technique.

1. Introduction

The stimulus for transparent electronics has galvanized the world-wide efforts to search for novel p-type transparent conducting oxide (TCO) thin-film materials; these should match with the presently available n-type counterparts for the fabrication of transparent electronic components such as p-n junction diodes. Transparent p-n and p-i-n junction diodes are important components for the realization of invisible electronics, and it is a common understanding that we already have a variety of prospective n-type TCOs in our hands but very few p-type materials of comparable characteristics.[1-4] Thus the research and development of p-type TCOs is a worthwhile endeavor not only to rival the current industry-standard n–type TCOs (e.g. Sn-doped In_2O_3 and Al-doped ZnO) but also to complement the needs of invisible electronics. Materials with a wide bandgap (>3 eV), high electrical conductivity, high hole mobility and low fabrication cost along with considerable transparency would be ideal for the transparent electronics.

Frustrated magnetism due to the triangular crystal lattice was the early reason for the intense studies on delafossite oxides but the discovery of p-type electrical conductivity in transparent $CuAlO_2$ thin films in late 1990s swung the pendulum of research on delafossites to the invisible electronics.[5,6] Subsequently several other wide-bandgap triangular-lattice delafossites of monovalent copper such as $CuInO_2$, $CuScO_2$, $CuGaO_2$, $CuYO_2$ and most recently $CuBO_2$ have been investigated as p-type TCOs.[7-12]

Among the delafossites, $CuCrO_2$ is probably the most prospective p-type candidate for TCO applications with its bandgap of >3.0 eV, though the bandgap is debatable with contradictory findings of indirect and direct bandgap semi-conductivity.[13-16] In their

early bandgap study Benko and Koffyberg reported an indirect bandgap of 1.28 eV for $CuCrO_2$ with another indirect and a direct bandgap at 3.08 and 3.35 eV, respectively.[13] The most recent optical measurements encouragingly indicate $CuCrO_2$ to be transparent to visible light with the direct optical bandgap in the range of 2.95–3.30 eV.[17-19] However, the low electrical conductivity of $CuCrO_2$ is a serious drawback for its use in practical TCO applications. Thus some sort of substitution/doping scheme is inevitably required to push the Fermi level closer to the top of the valence band to improve the p-type electrical conductivity. In some delafossites such as $CuScO_2$ and $CuYO_2$, excessive oxygen has been observed to enhance the electrical conductivity but this hole-doping approach may not be feasible in the case of $CuCrO_2$ due to the smaller ionic radius of Cr^{3+} compared to those of Sc^{3+} and Y^{3+}. Fortunately, hole-doping through the aliovalent Mg^{2+}-for-Cr^{3+} substitution seems to significantly improve the electrical conductivity albeit leading to a lowered transmittance (30%) in the visible region.[20] Currently there are many other reports on improved electrical conductivity and transmittance in the visible region achieved with the Mg^{2+}-for-Cr^{3+} substitution.[21-25] Moreover, the 5% Mg-substituted $CuCrO_2$ has shown the highest electrical conductivity (220 S cm^{-1}) to date among the delafossite oxides, the value being much higher than those for e.g. $Cu(Y,Ca)O_2$, $Cu(Sc,Mg)O_2$, $Cu(Al,Mg)O_2$ (4 x 10^{-4} S cm^{-1}) and $Cu(In,Ca)O_2$ (2.8 x 10^{-3} S cm^{-1}) thin films.[26,7]

There are various methods reported for the preparation of Mg-substituted $CuCrO_2$ thin films, such as rf sputtering, pulsed laser deposition, and chemical solution deposition.[18,21-25,27-31] However, these techniques may not be vital for the

applications where a precise thickness control (of the order of sub-nanometer) over a large-area and/or nanostructured substrate is required.[32] In some thin-film works Mg-substitution levels as high as 12% have been reported, clearly contradicting to the very limited substitution levels reported for bulk samples.[21,33-36] Atomic layer deposition (ALD) is an advanced gas-phase thin-film deposition technique that affords precise film-thickness control owing to its unique deposition mechanism based on sequential and repeated exposures of precursor vapors that undergo self-limiting surface reactions.[37] Not only low deposition temperatures but ALD also offers the benefit of wafer-scale fabrication of various inorganic films, including oxides, nitrides, metals and chalcogenides.[38]

Electrical transport properties of $Cu(Cr,Mg)O_2$ are still not fully understood, partly due to various uncertainties in the composition/structure, oxygen non-stoichiometry, Mg substitution at the Cu site and spin-charge coupling effects at the Cr site.[39,40] Moreover it is observed that the electrical conductivity of Mg-substituted $CuCrO_2$ films strongly depend on the deposition conditions, specifically the O_2 partial pressure during the film deposition.[41] In many sputtering experiments, introduction of oxygen during the film growth was not enough to obtain the high-conductivity films albeit the improved film's transmittance.[42] In a similar study on Mg-substituted Cr_2O_3 films, it was observed that the mixed-valence state of Cr due to the Mg substitution depends on the oxygen partial pressure.[43] In some rare earth delafossite oxides an unusual spin-gap-like behavior have been observed with oxygen doping.[44] In $CuScO_2$ films a tradeoff between optical transmittance and electrical conductivity was observed for post-

deposition O_2-annealed films, such that the electrical conductivity increased at the cost of the optical transmittance.[8,45] In view of the aforementioned findings and discussions, it is scientifically worthwhile and technologically highly desired to develop a feasible ALD route to deposit high-quality Mg-substituted $CuCrO_2$ thin films.

Continuing our recent success in developing a promising ALD process for high-quality non-substituted $CuCrO_2$ thin films, here in the present contribution we demonstrate the highly controllable Mg-for-Cr substitution in ALD-$CuCrO_2$ thin films.[46] We moreover report the optical bandgap for our $Cu(Cr,Mg)O_2$ films determined from UV-vis spectrophotometric measurements, and also the electrical transport properties (electrical resistivity and Seebeck coefficient) for the films having the eye on their potential optoelectronic device applications such as flat-panel displays and photovoltaics. It is anticipated that for these applications materials should exhibit the high optical transmittance (>80%) of incident light and the high electrical conductivity (>10^3 S cm^{-1}) for efficient carrier transport. The optical transmittance and electronic conduction of thin films in general do get limited by the scattering of photons and charge carriers at the defects and grain boundaries. Hence the employment of ALD may prove useful for optoelectronic applications with the nearly defect-free and homogeneous film growth.

2. Results and Discussion

In Figure 1(a) we show the GIXRD patterns and AFM images for our $Cu(Cr_{1-x}Mg_x)O_2$ films with the nominal Mg content x up to 0.043, after annealing the as-deposited films in Ar gas at 800 °C. As has been observed for many ALD-grown ternary oxide films the as-deposited films were non-crystalline and required the heat treatment for the

crystallization; after the heat treatment all the films were well crystalline. From Figure 1(a), it is observed that up to $x \approx 0.01$ the films seem to be of the pure delafossite phase but for $x \geq 0.015$ some extra peaks appear that correspond to a spinel structure. The main (311) peak of the spinel phase and the (101) and (012) peaks of the delafossite phase strongly overlap such that it is difficult to distinguish them. However, evolution of several other peaks of the spinel phase with increasing x could be readily monitored; from the peaks detected it was not possible to determine whether the spinel phase is $CuCr_2O_4$ (JCPDS 00-26-0509) or $MgCr_2O_4$ (JCPDS 00-10-0351) or their mixture as the diffraction patterns of the two phases are almost identical. However, from literature it is known that $CuCr_2O_4$ gets converted to $CuCrO_2$ when annealed at temperatures higher than 700 ^oC.[25] Hence, we tentatively assume that the secondary phase in our thin films is $MgCr_2O_4$ or $(Mg,Cu)Cr_2O_4$. From Figure 1(a), the relative content of the spinel phase increases with increasing Mg content for $x \geq 0.015$; unfortunately it is not possible to more precisely quantify the amount of the spinel phase based on the GIXRD data.

The AFM images for the as-deposited non-crystalline films (not shown here) revealed very smooth homogeneous surfaces with surface roughness (RMS; root mean square) values <1 nm; upon the annealing when the films become crystalline the RMS value increases, as shown in Figure 1(b). Finally for the higher nominal Mg contents the RMS value slightly decreases/saturates. This seems to coincide with the emergence of the spinel secondary phase.

There are several papers for both thin-film and bulk samples of $Cu(Cr,Mg)O_2$ where even Mg-substitution levels greater than 10% have been reported.[14, 21, 25] However,

from a recent experimental and theoretical investigation by Maignan et al.,[33] a very limited solubility range up to ~1% was concluded for bulk $Cu(Cr,Mg)O_2$ samples. Maignan et al. also identified the spinel impurity phase as $MgCr_2O_4$.[33] To ascertain the solid solubility of Mg in our $Cu(Cr_{1-x}Mg_x)O_2$ thin films we take in Figure 1(c) a closer look at the GIXRD patterns on an expanded scale around the sharpest peak (006). A shift in the peak position towards the lower angles is observed with increasing x that indicates the increase in the unit cell. As shown in the inset of Figure 1(c), with increasing nominal Mg content x, an initial rapid shift in the peak position towards the lower angles (i.e. increase in lattice parameter c) is followed by saturated/very slowly increasing c parameter after $x \approx 0.025$. Hence we conclude that initially all Mg goes to the delafossite matrix up to $x \approx 0.015$ after which a portion of the added Mg precipitates as the spinel phase. Nevertheless, from the lattice parameter behavior it seems that even after the spinel phase starts to precipitate some Mg is still dissolved in the delafossite phase. A similar behavior for the increase in lattice parameter c was reported by Okuda et al. for polycrystalline Mg-doped $CuCrO_2$ bulk samples.[34, 35] As the ionic radius of Mg^{2+} (0.720 Å) is larger than that of Cr^{3+} (0.615 Å), our observations for the continuous but not linear increases in lattice parameter c up to $x \approx 0.025$ provide clear evidence for the solubility of Mg on the octahedral delafossite site in our ALD-grown $Cu(Cr_{1-x}Mg_x)O_2$ thin films, but the exact extent of solubility remains somewhat ambiguous.[47]

In Figure 2 we first plot the room-temperature electrical resistivity (ρ) and Seebeck coefficient (S) values as a function of x for our $Cu(Cr_{1-x}Mg_x)O_2$ films (upper figure), and then show the temperature dependence

of ρ and S in the lower figure for the x = 0.035 film. Firstly, the temperature dependence of resistivity shows a purely semiconducting behavior with dr /dT < 0, and the positive Seebeck values confirm the p-type electrical conductivity. The activation energy calculated from the plot of log r versus 1000/T (not shown here) yields activation energy values of 260, 186 and 120 meV for x = 0.0, 0.025 and 0.035, respectively. These values are much higher than the one (20 meV) reported by Nagarajan et al.,[20] but comparable to those (292, 187 and 87 meV for x = 0.0, 0.02 and 0.04, respectively) reported by Han et al. for their $Cu(Cr_{1-x}Mg_x)O_2$ films.[21] The estimated activation energies are much smaller than half of the bandgap, which indicates that the hole transport in the valence band is thermally activated from an acceptor. Apparently Mg-doping lowers the Fermi level on the top of the valence band, such that the carriers can easily jump to the Fermi level from the valence band.

The room-temperature S values are similar to those reported in literature for both bulk and thin-film $Cu(Cr,Mg)O_2$ samples. However, for our ALD thin films dS/dT < 0, which is in contrast to the behavior reported for bulk samples.[33] With increasing nominal Mg content x, the room-temperature ρ and S values both decrease sharply up to x = 0.015 and then get essentially saturated before increasing slightly for the x = 0.043 sample. These observations are essentially in line with our tentative conclusions for the solubility of Mg in the delafossite phase based on the GIXRD results. The slightly increased ρ and S values for x = 0.043 may be related to the presence of the spinel phase in quantities able to block the percolation paths of electrical conduction. The initial decrease in electrical resistivity and Seebeck coefficient upon increasing x is ascribed to

the hole (i.e. Cr^{4+}) creation at the chromium site due to the aliovalent Mg^{2+}-for-Cr^{3+} substitution; the Cr^{3+}/Cr^{4+} mixed valency is widely considered as responsible for the transport properties in the Cr-based delafossite phases.[33] There are also some conflicting reports assuming hole creation at the copper site (i.e. Cu^{2+}).[34,35] However, Maignan et al. ruled out this possibility through careful magneto-thermoelectric measurements.[33]

The highest electrical conductivity of 217 S cm^{-1} for our ALD-grown x = 0.025 thin-film sample is of the very same level as the highest value of 220 S cm^{-1} so far reported for $Cu(Cr,Mg)O_2$ thin films, and much higher than the values typically achieved, i.e. 1~50 S cm^{-1}, for such films (see Table 2 for comparison).[20,21,25-28] The relatively large discrepancy in the electrical conductivity values reported by different groups must be due to the different preparation conditions, in particular the oxygen partial pressure. However the literature data are somewhat conflicting in terms of the effects of oxygen pressure, as in some reports the films prepared in an oxygen-deficient atmosphere show high electrical conductivity but low transmittance and in some cases just the opposite has been observed.[8, 20, 41-45, 48] Nevertheless, it is widely believed that the presence of interstitial oxygen in $Cu(Cr,Mg)O_2$ thin films could improve the electrical conductivity due to hole doping.[5,10,43,44] This could be true in our case as well, as in our ALD deposition process ozone gas as a source for oxygen is pulsed into the reactor in every ALD cycle.

Recently it was revealed that the Fermi-level structure near the valence band maximum has both Cu 3d and Cr 3d characters through Cu 3d –O 2p–Cr 3d hybridization.[49,50] With increasing Mg doping, Cu^{2+} defect states could increase as a consequence of the

increasing amount of holes introduced into the upper part of the valence band. This would disturb the up-spin configuration of Cr 3d orbitals and greatly impede the dispersion of the 3d states,[21] thereby prohibiting the electrical conductivity increase. Most likely this is not the case in our films, though.

For the further confirmation of the type of electrical conductivity and estimation of the charge carrier density, we performed Hall coefficient measurements on some of our samples. The Hall coefficient was confirmed to be positive, being 0.1035, 0.0287 and 0.0143 cm^{-3}/Coulomb for our x = 0.01, 0.025 and 0.035 thin films, respectively. The positive value of Hall coefficient thus verifies the p-type conductivity, in line with the conclusion made from the Seebeck coefficient measurements. For the same samples, the carrier concentration was calculated to be 6.04×10^{19}, 2.17×10^{20} and 4.35×10^{20} cm^{-3}, respectively, from the Hall coefficient measurements. These values match well to the values reported in literature.[14,22,24,27,35]

The UV-vis spectra measured in the wavelength range 190-1100 nm for our 120-150 nm thick $Cu(Cr_{1-x}Mg_x)O_2$ thin films are displayed in Figure 3. In conciliation with the AFM data, the transmittance of the films follows exactly the opposite trend to the surface roughness (see inset of the upper figure). The maximum optical transmittance of close to ~80% in the wavelength range 600–800 nm is observed for the x = 0.035 film. Most importantly, for the x = 0.025 film with the highest electrical conductivity the transmittance is >70%, that is, more than twice the transmittance value (30%) achieved by Nagarajan et al. for their highest conducting $Cu(Cr,Mg)O_2$ films deposited by the PLD technique.[20] In general, our transmittance values are better than the

values reported in literature for $CuCrO_2$ and $Cu(Cr,Mg)O_2$ films (60-75%) deposited by any other technique, see Table 2.[20,21,51] The optical bandgap increases even after x = 0.015, i.e. at the point where the spinel secondary-phase starts to form.

We calculated the absorption coefficient a and the optical bandgap of the films in a way earlier reported by us for the parent $CuCrO_2$ films.[46] The middle and bottom insets of Figure 3 show the absorption coefficient as a function of wavelength and the bandgap as a function of x, respectively. The absorption curves rise sharply (characteristic absorption) around 400 nm and similarly to the parent $CuCrO_2$ phase show a peak (marked as I) located around 350 nm corresponding to incident photon energy of 3.54 eV. It is discussed in literature that such peaks may appear due to sub-bandgap transitions, when the relationship, $h\nu = E_g - E_k$ between an incident photon and a free exciton (bound state of an electron and a hole) in a semiconductor is satisfied.[52-55] Here hn is the incident photon energy, E_g is the bandgap and E_k is the binding energy of the free exciton and k represents the wave-vector on the E–k diagram; on this diagram, sub-bands lie at the lower energy positions. Thus sub-bandgap transitions are not in general capable of creating hole- carriers to make any appreciable contribution to the electrical conductivity. As shown in Figure 3 the direct bandgap for our ALD $Cu(Cr_{1-x}Mg_x)O_2$ films is estimated from 3.09 eV for x = 0 to 2.87 eV for x = 0.015 before further increasing to 3.15 eV for x = 0.43. The obtained values are consistent with direct bandgaps of 2.95–3.55 eV reported in previous studies.[21-25] This initial decrease followed by an increase in the bandgap energy was observed in another work as well,[21] where it was explained by the bandgap renormalization and Burstein-Moss

effect. Keeping in mind the debate about the nature of the bandgap we also plot the indirect bandgap for our thin films, as shown in the inset of Figure 3. The indirect bandgap values follow a similar trend as observed for the direct one, changing from 2.35 to 2.78 eV. These values are consistent with the indirect bandgaps reported in literature.[13-16]

Finally, we like to emphasize that the p-type electrical conductivity in $Cu(Cr,Mg)O_2$ has been the point of intense debate because of the following two reasons: (1) this phase shows the highest p-type electrical conductivity among delafossite oxides, and (2) the results revealed for it contradict the common trend seen for several other delafossite phases $CuMO_2$ (M = B, Al, Sc, Y), i.e. the decrease in electrical conductivity with increasing size of the M^{3+} cation due to the increased Cu-Cu distance. The p-type electrical conductivity of these delafossites is subject to three kinds of defects, namely copper vacancies (V_{Cu}), oxygen interstitials (O_i), and dopants on the M lattice site (in the present case Mg on the Cr lattice site). Copper vacancies are discussed mainly to understand the conductivity of pure delafossites,[17] while for the cation-doped systems, dopants and O_i play the main roles. The interplay of these different doping schemes then most probably account for the complexity of the electrical transport and optical properties of the different delafossite phases.

3. Conclusions

In this work, we developed an ALD process based on $Cu(thd)_2$, $Cr(acac)_3$ and $Mg(thd)_2$ metal precursors and ozone as the oxygen source to fabricate high-quality $Cu(Cr_{1-x}Mg_x)O_2$ thin films; in our depositions the proper sequence of the sub-cycles for each metal constituent was found to get the desired Cu/Cr/Mg ratio in the films. The

information of the process parameters may also be useful for the deposition of other members of the $CuBO_2$ delafossite family with different B-site constituents (e.g. Al, Mn) for potential TCO applications. From GIXRD measurements the observed limited substitution limit of around 2% is consistent with values reported for bulk samples in literature. The as-deposited films were non-crystalline and exhibited smooth homogeneous surfaces; annealing at 800 °C in an Ar atmosphere then resulted in well-crystalline $Cu(Cr,Mg)O_2$ films with promising TCO characteristics.

Transport property measurements (electrical resistivity, Seebeck and Hall coefficient) confirmed the p-type semiconducting behavior for the films. Most importantly, we verified the highest optical transmittance values up to >80% in the visible range along with the appreciably high electrical conductivity values up to 217 S cm^{-1}. The direct bandgap was determined at 2.87-3.15 eV for the films. Though there are some reports that divalent cation substitutions (e.g. Mg, Ca) could increase the electrical conductivity of other delafossite compounds as well, the Mg-substituted $CuCrO_2$ is yet the most promising p-type TCO material candidate among the delafossites, not only to its superior electrical properties but also owing to its excellent thermal stability.

4. Experimental Section

Magnesium-for-chromium substituted thin films of $Cu(Cr_{1-x}Mg_x)O_2$ with x = 0.0–0.043 were deposited from Cu(thd)2 (thd = 2,2,6,6-tetramethyl-3,5-heptanedionate), $Mg(thd)_2$) and $Cr(acac)_3$ (acac = acetyl acetonate) as metal precursors and ozone as the source for oxygen. For the depositions the commercial hot-wall flow-type F-120 ALD reactor (ASM Microchemistry Ltd., Finland) was employed with an operational nitrogen pressure of 2-3

mbar. NITROX UHPN 3000 nitrogen generator was used to produce high-purity nitrogen (99.9995%) gas which was used both as a carrier and purging gas. The precursors $Cr(acac)_3$ (97.5%) and $Mg(thd)_2$ (98%) were procured from STREM chemicals, whereas the copper precursor $Cu(thd)_2$ was prepared from copper acetate (Fluka; 98%) and 2,2,6,6-tetramethyl hepatane-3,5-dione (Fluka; >98%) in our laboratory. The ozone gas which is more reactive than oxygen in the depositions was produced with a Fischer model 502 laboratory ozone generator from oxygen (99.999%). It was pulsed into the reactor through a combination of needle and solenoidal valves connected to the main ozone flow line.

In the depositions all the precursors were sublimed from open glass boats held inside the reactor at 120, 130 and 150 ^{0}C, for $Cu(thd)_2$, $Cr(acac)_3$ and $Mg(thd)_2$, respectively. These sublimation temperatures were selected based on thermogravimetric (TG) analysis (carried out in air with a heating rate of 10 ^oC/min) and also on our previous experience. The deposition parameters such as the pulse/purge lengths for $Cu(thd)_2$, $Cr(acac)_3$ and O_3, and the deposition temperature (250 ^oC) were kept the same as those reported by us in our recent publication for the deposition of the parent $CuCrO_2$ films.[44] The pulse/purge lengths for $Mg(thd)_2$ were fixed at 2 s/3 s similarly to those for $Cu(thd)_2$ and $Cr(acac)_3$. To realize the Mg substitution in the films we replaced a certain number of $Cr(acac)_3+O_3$, sub-cycles by $Mg(thd)_2+O_3$ sub-cycles for the desired Mg-substitution level. In all the depositions the following deposition cycle was utilized: $N*[n*\{Cu(thd)_2+O_3) + 3*(Cr(acac)_3+O_3)\} + \{(Cu(thd)_2+O_3) + 2*((Cr(acac)_3+O_3)\} + (Mg(thd)_2+O_3)\}]$. Here N is the number of substitution-cycles and n is the number of

super-cycles similar to the $CuCrO_2$ depositions. In other words, for each substitution-cycle N there are n super-cycles and one extra super-cycle where one sub-cycle of chromium ($Cr(acac)_3$+O_3) is replaced by a sub-cycle for magnesium ($Mg(thd)_2$+O_3). In all the depositions the number N*n was fixed to 300 to deposit thin films of similar thickness. The linear ALD growth behavior was observed as the main growth cycle (i.e. n; super-cycle) for $CuCrO_2$ was still the dominant cycle. The nominal Mg-substitution level could then be calculated from the formula, N/(N*n*3+2*N). For example when the substitution-cycle N is 3 and super-cycle n is 100 we will have the substitution level of x = 0.003; for the other x values, the corresponding N and n values are given in Table 1. Wavelength-dispersive X-ray fluorescence spectroscopy measurements (WD-XRF; PANanalytical Axios^{mAX} microanalysis system equipped with SST-mAX X-ray tube that virtually eliminates instrument drift) were then employed to confirm the elemental composition of the films. SuperQ software package from PANanalytical was used for the analysis of the XRF results.

As was observed by us for pure $CuCrO_2$ and many other ternary oxides, the as-deposited films were amorphous; thus for crystallization the films were annealed at 800 ^oC in a rapid thermal annealing (RTA) furnace PEO 601 (ATV Technologie GmbH) in an Ar atmosphere for 10 minutes.[56-59] All the films were deposited on 3.5 × 3.5 cm^2 borosilicate glass substrates for the purpose of bandgap determination from UV-vis spectrophotometric and electrical transport measurements. The spectrophoto-metric measurements were performed by Hitachi-U 2000 spectrophotometer in the wavelength range of 190-1100 nm. PANanalytical (X'pert Pro diffractometer; CuK_α) diffractometer

was used to determine the thickness of the as-deposited films from X-ray reflectivity (XRR) measurements and the crystal structure of the annealed films from the grazing-incidence X-ray diffraction (GIXRD; grazing-incidence angle 0.5^0). Atomic force microscopy (AFM; TopoMetrix Explorer) images were taken to investigate the surface roughness and morphology of the films. DC electrical resistivity (r) was measured for the annealed films in linear four-probe configuration whereas the Seebeck coefficient (S) was measured using our home-made setup reported in reference.[60] Hall coefficient measurements were performed at room temperature using a 1 Tesla electromagnet and Van der Pauw geometry for the Hall voltage measurement.

Acknowledgment

The present work has received funding from the European Research Council under the European Union's Seventh Framework Programme (FP/2007-2013)/ERC Advanced Grant Agreement (No. 339478) and also from the Aalto Energy Efficiency Research Programme.

[1] Antonio Facchetti, Tobin Marks, Transparent Electronics: From Synthesis to Applications, John Wiley & Sons, 2010.

[2] A. Kudo, H. Yanagi, H. Hosono, H. Kawazoe, *Appl. Phys. Lett.* 1998, 73, 220.

[3] Y. W. Heo, Y. W. Kwon, Y. Li, S. J. Pearton, D.P. Norton, *Appl. Phys. Lett.* 2004, 84, 3474.

[4] H. S. Kim, S. J. Pearton, D. P. Norton, F. Ren, *J. Appl. Phys.* 2007, 102, 104904.

[5] H. Kawazoe, M. Yasukawa, H. Hyodo, M. Kurita, H. Yanagi, H. Hosono, *Nature (London)* 1997, 389, 939.

[6] G. Thomas, *Nature (London)* 1997, 389, 907.

[7] H. Yanagi, T. Hase, S. Ibuki, K. Ueda, H. Hosono, *Appl. Phys. Lett.* 2001, 78, 1583.

[8] N. Duan, A. W. Sleight, M. K. Jayaraj, J. Tate, *Appl. Phys. Lett.* 2000, 77, 1325.

[9] H. Kawazoe, H. Yanagi, K. Ueda, H. Hosono, *MRS Bull.,* 2008, 25, 28.

[10] R. Nagarajan, N. Duan, M. K. Jayaraj, J. Li, K. A. Vanaja, A. Yokochi, A. Draeseke, J. Tate, A. W. Sleight, *Int. J. Inorg. Mater.* 2001, 3, 265.

[11] M. Snure, A. Tiwari, *Appl. Phys. Lett.* 2007, 91, 092123.

[12] D. O. Scanlon, A. Walsh and G. W. Watson, *Chem. Mater.* 2009, 21, 4568.

[13] F. A. Benko, F. P. Koffyberg, *Mater. Res. Bull.* 1986, 21, 753.

[14] A. C. Rastogi, S. H. Lim, S. B. Desu, *J. Appl. Phys.* 2008, 104, 023712.

[15] S. Mahapatra, S. A. Shivashankar, *Chem. Vap. Deposition* 2003, 9, 238.

[16] D. Li, X. Fang, Z. Deng, S. Zhou, R. Tao, W. Dong, T. Wang, Y. Zhao, G. Meng, X. Zhu, *J. Phys. D: Appl. Phys.* 2007, 40, 4910.

[17] D. O. Scanlon, G. W. Watson, *J. Mater. Chem.* 2011, 21, 3655.

[18] W. T Lim, L. Stafford, P. W. Sadik, D. P. Norton, S. J. Pearton, Y. L. Wang, F. Ren, *Appl. Phys. Lett.* 2007, 90, 142101.

[19] S. Zhou, X. Fang, Z. Deng, D. Li, W. Dong, R. Tao, T. Meng, X. Zhu, *J. Cryst. Growth* 2008, 310, 5375.

[20] R. Nagarajan, A. D. Draeseke, A. W. Sleight, J. Tate, *J. Appl. Phys.* 2001, 89, 8022.

[21] M. J. Han, Z. H. Duan, J. Z. Zhang, S. Zhang, Y. W. Li, Z. G. Hu, J. H. Chu, *J. Appl. Phys.* 2013, 114, 163526.

[22] X. R. Li, M. J. Han, P. Change, Z. G. Hu, Y. W. Li, Z. Q. Zhu, J. H. Chu, *Appl. Phys. Lett.* 2014, 104, 012103.

[23] X. R. Li, M. J. Han, P. Change, Z. G. Hu, Y. W. Li, Z. Q. Zhu, J. H. Chu, *Phys. Rev. B.* 2014, 90, 053308.

[24] R. Bywalez, S. Götzendörfer, P. Löbmann, *J. Mater. Chem.* 2010, 20, 6562.

[25] S. H. Lim, S. Desu, and A. C. Rastogi, *J. Phys. Chem. Solids* 2008, 69, 2047.

[26] M. A. Marquardt, N. A. Ashmore, D. P. Cann, *Thin Solid Films* 2006, 496, 146.

[27] A. Barnabé, Y. Thimont, M. Lalanne, L. Presmanes, P. Tailhades, *J. Mater. Chem. C* 2015, 3, 6012.

[28] P. W. Sadik, M. Ivill, V. Craciun, D. P. Norton, *Thin Solid Films* 2009, 517, 3211.

[29] S. Y. Kim, S. Y. Sung, K. M. Jo, J. H. Lee, J. J. Kim, S. J. Pearton, D. P. Norton, Y. W. Heo, *J. Cryst. Growth* 2011, 326, 9.

[30] D. Li, X. Fang, Z. Deng, W. Dong, R. Tao, S. Zhou, J. Wang, T. Wang, Y. Zhao, X. Zhu, *J. Alloys Compd.* 2009, 486, 462.

[31] L. Xurui, H. Meijie, Z. Xiaolong, S. Chao, H. Zhigao, Z. Ziqiang, C. Junhao, *Phys. Rev. B* 2014, 90, 035308.

[32] S.-Å. Lindgren, L. Walldén, Chapter 13 of *Electronic Structure* (Handbook of Surface Science) volume 2, *Some Properties of Metal Overlayers on Metal Substrates,* Newnes, 2000.

[33] A. Maignan, C. Martin, R. Frésard, V. Eyert, E. Guilmeau, S. Hébert, M. Poienar, D. Pelloquin, *Solid State Commun.* 2009, 149, 962.

[34] T. Okuda, Y. Beppu, Y. Fujii, T. Onoe, N. Terada, S. Miyasaka, *Phys. Rev. B* 2008, 77, 134423.

[35] T. Okuda, N. Jufuku, S. Hidaka, N. Terada, *Phys. Rev. B* 2005, 72, 144403.

[36] Y. Ono, K. Satoh, T. Tomohiro Nozaki, T. Kajitani, *Jpn. J. Appl. Phys*. 2007, 46, 1071.

[37] G. N. Parsons, J. W. Elam, S. M. George, S. Haukka, H. Jeon, W. M. M. Kessels, M. Leskelä, P. Poodt, M. Ritala, S. M. Rossnagel, *J. Vac. Sci. Technol. A* 2013, 31, 050818.

[38] Hwang Cheol Seong, *Atomic Layer Deposition for Semiconductors,* Springer Science & Business Media, 2013.

[39] D. J. Aston, D. J. Payne, A. J. H. Green, R. G. Egdell, D. S. L. Law, J. Guo, P. A. Glans, T. Learmonth, K. E. Smith, *Phys. Rev. B* 2005, 72, 195115.

[40] M. V. Lalić, J. Mestnik-Filho, A. W. Carbonari, R. N. Saxena, *Solid State Commun.* 2003, 125, 175.

[41] T. Minami, H. Tanaka, T. Shimakawa, T. Miyata, *Proc. SPIE* 2004, 5274, 399–406.

[42] T. Minami, *Semicond. Sci. Technol.* 2005, 20, S35.

[43] N. Uekawa, K. Kaneko, *J. Phys. Chem.* 1996, 100, 4193.

[44] K. Isawa, Y. Yaegashi, M. Komatsu, M. Nagano, S. Sudo, *Phys. Rev. B* 1997, 56, 3457.

[45] J. Tate, M. K. Jayaraj, A. D. Deaeseke, T. Ulbrich, A. W. Sleight, K. A. Vanaja, R. Nagarajan, J. F. Wager, R. L. Hoffman, *Thin Solid Films* 2002, 411, 119.

[46] T. S. Tripathi, J.-P. Niemelä, M. Karppinen, *J. Mater. Chem. C* 2015, 3, 8364.

[47] M. Lalanne, A. Barnabé, F. Mathieu, Ph. Tailhades, *Inorg. Chem.* 2009, 48, 6065.

[48] M. K. Jayaraj, A. D. Draeseke, J. Tate, A. W. Sleight, *ThinSolidFilms* 2001, 397, 244.

[49] T. Yokobori, M. Okawa, K. Konishi, R. Takei, K. Katayama, S. Oozono, T. Shinmura, T. Okuda, H. Wadati, E. Sakai, K. Ono, H.

Kumigashira, M. Oshima, T. Sugiyama, E. Ikenaga, N. Hamada, and T. Saitoh, *Phys. Rev. B* 2013, 87, 195124.

[50] D. O. Scanlon, A. Walsh, B. J. Morgan, G. W. Watson, D. J. Payne, and R. G. Egdell, *Phys. Rev. B* 2009, 79, 035101.

[51] H.-Y. Chen, K.-P. Chang, *ECS J. Solid State Sci. Technol.* 2013, 2, P76.

[52] F. Bassani, G. P. Parravicini, *Electronic States and Optical Transitions in Solids*, Pergamon, Oxford, 1975.

[53] R. S. Yu, C. M. Wu, *Appl. Surf. Sci.* 2013, 282, 92.

[54] G. L. Li, and Z. Yin, *Phys. Chem. Chem. Phys.* 2011, 13, 2824.

[55] J. I. Pankove, *Optical Processes in Semiconductors,* Prentice-Hall Inc., Englewood Cliffs, NJ, 1971.

[565] K. Uusi-Esko, J. Malm, M. Karppinen, *Chem. Mater.* 2009, 21, 5691.

[57] K. Uusi-Esko, E.-L. Rautama, M. Laitinen, T. Sajavaara, M. Karppinen, *Chem. Mater*. 2010, 22, 6297.

[58] E. Ahvenniemi, M. Matvejeff, M. Karppinen, *Dalton Trans*. 2015, 44, 8001.

[59] K. Uusi-Esko, M. Karppinen, *Chem. Mater.* 2011, 23, 1835.

[60] T. S. Tripathi, M. Bala, K. Asokan, *Rev. Sci. Instrum.* 2014, 85, 085115.

[61] Z. Xiaoshan, L. Fangting, S. Wangzhou, L. Aiyun, *Journal of Alloysand Compounds* 2014, 614, 221.

[62] J. Crepelliere, P. Lunca Popa, N. Bahlawane, R. Leturcq, F. Werner, S. Siebentritt and D. Lenoble, J. Mater. Chem. C, 2016, DOI: 10.1039/C6TC00383D.

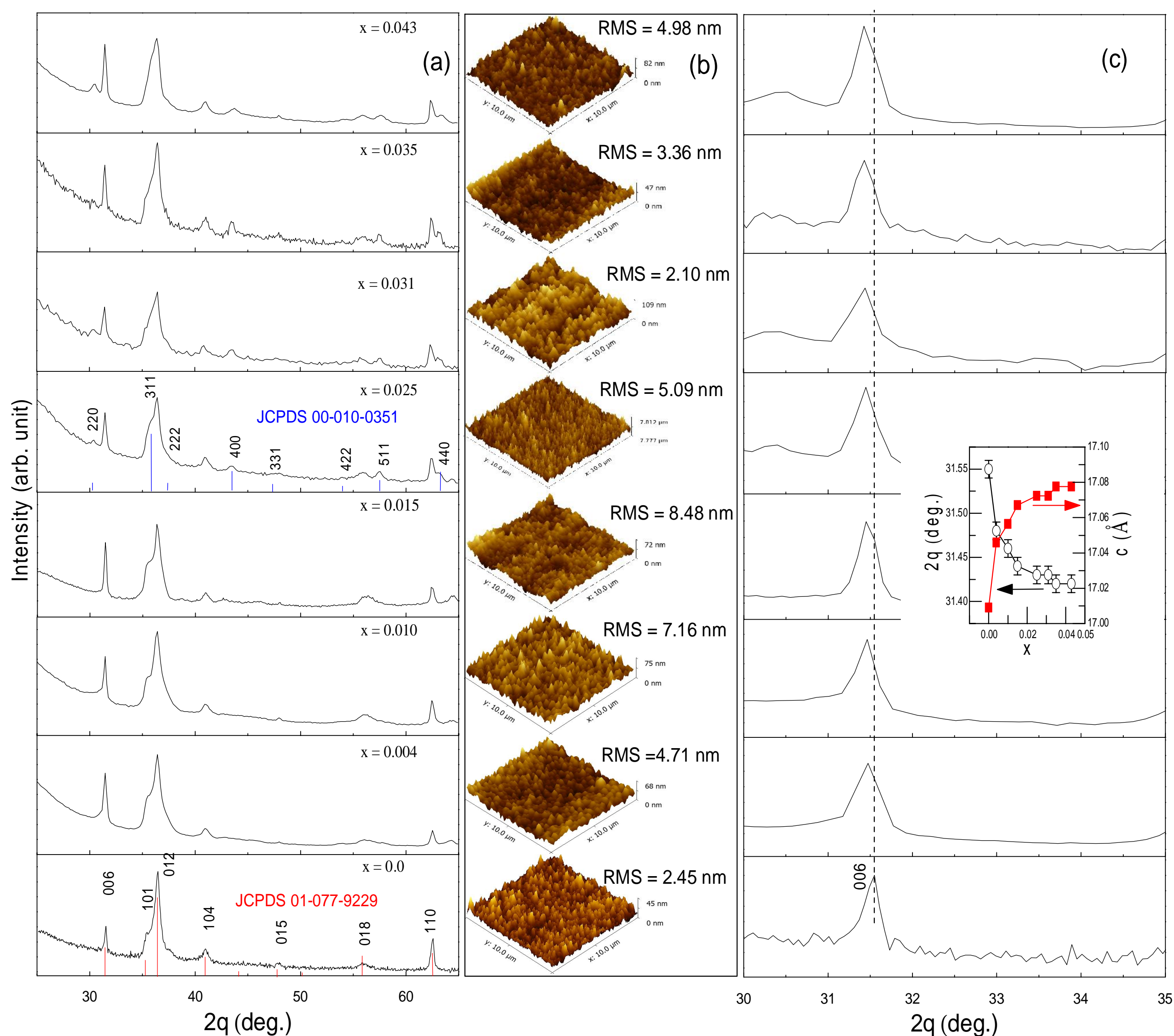

Figure 1. (a) GIXRD patterns and (b) AFM images for the $Cu(Cr_{1-x}Mg_x)O_2$ films taken after the as-deposited films had been annealed at 800 ^{0}C in Ar. Red and blue lines show the diffraction peaks from JCPDS reference data for $CuCrO_2$ (JCPDS 01-077-9229) and $MgCr_2O_4$ (JCPDS 00-010-0351), respectively. (c) GIXRD patterns for the films on an expanded scale around the peak (006). The inset shows the decrease in 2θ value and the corresponding increase in lattice parameter c with increasing x calculated for the hexagonal delafossite structure.

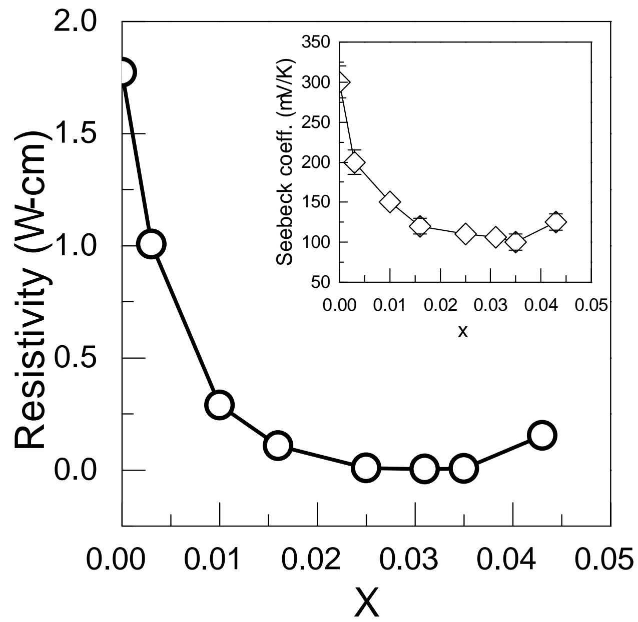

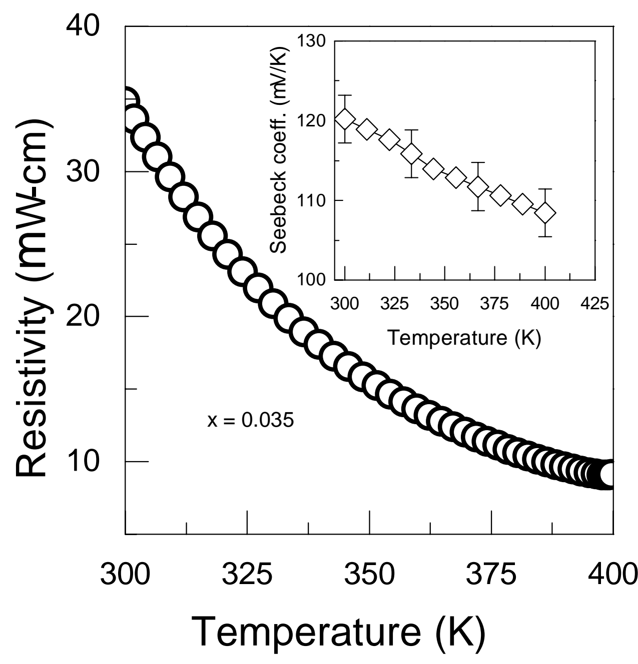

Figure 2. Room-temperature electrical resistivity and Seebeck coefficient (inset figures) data for the $Cu(Cr_{1-x}Mg_x)O_2$ films as a function of Mg-substitution level x (upper panel) and temperature for the x = 0.035 sample (lower panel).

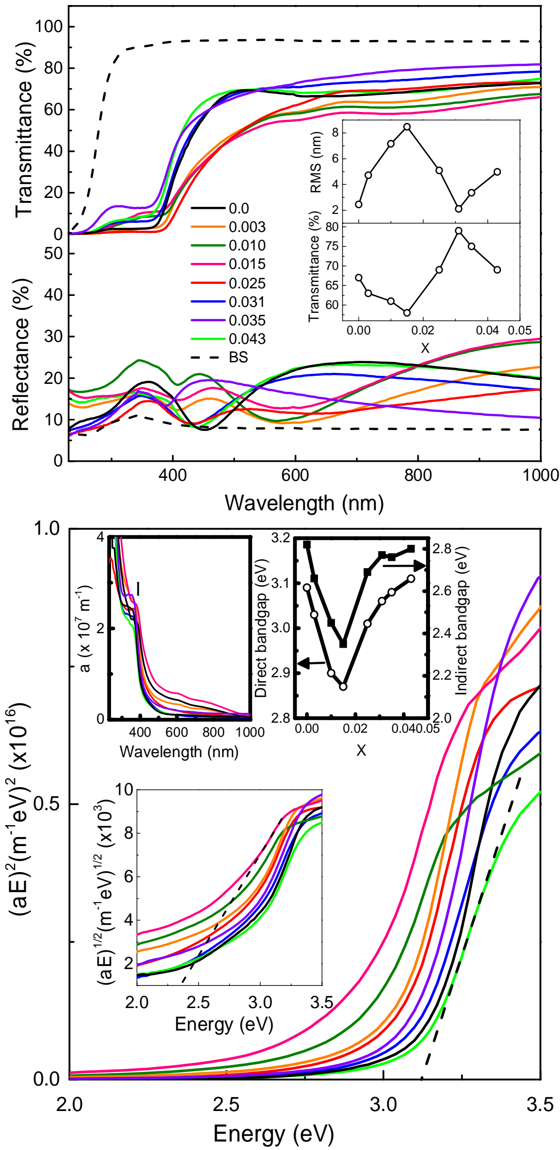

Figure 3. (Upper) Transmittance and reflectance spectra for the $Cu(Cr_{1-x}Mg_x)O_2$ films; the inset compares the trends in the RMS roughness and transmittance values with increasing x. (Lower) Determination of the direct bandgap for the films; the insets show the indirect bandgap as a function of energy, absorption coefficient as a function of wavelength and the direct and indirect bandgaps as a function of x.

Table 1. Different values for the number of substitution cycles (N) and super-cycles (n) applied in the depositions, and the resultant Mg-substitution level, x.

Substitution cycle (N)	Super-cycle (n)	x	
		Nominal from N/(N*n*3+2*N)	Experimental from XRF
3	100	0.003	0.0038
10	30	0.010	0.0107
15	20	0.016	
25	12	0.025	0.027
30	10	0.031	
35	9	0.034	
40	7	0.043	0.044

Table 2. Room-temperature electrical transport properties and optical properties in the visible spectral range reported by others and by us.

Compound	Maximum substitution level (x)	S (mV/K)	s (S/cm)	Direct bandgap (eV)	Transmittance in visible range (%)	References
$CuCrO_2$	0	+300	1-17	3.09-3.13	50-75	[46, 61, 62]
$Cu(Cr_{1-x}Mg_x)O_2$	0.025	+120	217	3.0	70	This work
$Cu(Cr_{1-x}Mg_x)O_2$	0.03	+121	1.6	3.30	69	[27]
$Cu(Cr_{1-x}Mg_x)O_2$	0.05	+153	220	3.10	40-50	[10,20]
$Cu(Cr_{1-x}Mg_x)O_2$	0.07	+70	0.6-1	3.08-3.11	>80	[14, 25]
$Cu(Mn_{1-x}Mg_x)O_2$	0.15	NA	0.083	3.16	70	[61]
$Cu(Y_{1-x}Ca_x)O_2$	0.02	+275	1	3.50	50	[48]
$Cu(Sc_{1-x}Mg_x)O_2$	0.05	+100	20	NA	20	[45]
$Cu(In_{1-x}Ca_x)O_2$	0.07	+480	$2.8x10^{-3}$	3.90	70	[7]

TOC Figure